RSC Advances

ROYAL SOCIETY OF CHEMISTRY

www.rsc.org/advances

Journal Name

COMMUNICATION

Mesoporous Co_3O_4 @ Carbon Composites Derived from Microporous Cobalt-Based Porous Coordination Polymers for Enhanced Electrochemical Properties in Supercapacitors

Received 00th January 20xx,
Accepted 00th January 20xx

DOI: 10.1039/x0xx00000x

www.rsc.org/

Shuang Wang, Ting Wang, Ying Shi, Guang Liu, and Jinping Li*

In this work, mesoporous Co_3O_4 @ carbon composites were prepared through a simple, one-step, carbonization of microporous cobalt-based porous coordination polymers ZSA-1. After the carbonization, the original octahedral shape of the precursors ZSA-1 has been well preserved, and the obtained octahedrons were consisting of irregular nanoparticles with an average size of 10 nm. The as-synthesized Co_3O_4 @ carbon composites displayed mesoporous apertures with an average pore size of 3.6 nm. The octahedral Co_3O_4 @ carbon composites were evaluated as an electrode material of supercapacitors by cyclic voltammetry (CV) and galvanostatic charge/discharge tests. The electrochemical results show that the mesoporous Co_3O_4 @ carbon composites exhibiting a specific capacitance of 205.4 $F{\cdot}g^{-1}$ at a current density of 0.2 $A{\cdot}g^{-1}$. Furthermore, the characterization of mesoporous Co_3O_4 @ carbon composites was fully developed, including powder X-ray diffraction, scanning electron microscopy, transmission electron microscopy, N_2 adsorption, thermal gravimetric analyses, and Raman spectroscopy.

Introduction

With the rapid development of the global economy, the up-coming depletion of fossil fuels, and ever-increasing environmental problems, there is an urgent need for efficient, clean, and sustainable sources of energy, as well as new technologies associated with energy conversion and storage [1, 2]. Electrochemical capacitors (ECs), also known as supercapacitors or ultracapacitors, are essential components of high-rate electric devices used in the development of hybrid vehicles [3, 4]. Generally, on the basis of the energy storage mechanism, supercapacitors can be classified into two categories: (i) The Electrical Double-Layer Capacitors (EDLCs), which store charges electrostatically via reversible ion absorption at the electrode/electrolyte interface [5-7]; (ii) The Pseudo-Capacitors, where an actual battery-type oxidation-reduction reaction occurs leading to the pseudo-capacitance [8-10]. Active materials in electrodes of supercapacitors have great effects on electrochemical performance and capacity of energy storage devices, and looking for new electrode materials has become a key issue for the supercapacitor development. In general, carbon materials including porous carbon, CNTs, and grapheme are commonly studied as electrodes for EDLCs due to their good processing ability, large surface area, high porosity, good cycle life, and low cost [11-13]. Transition metal oxides (like RuO_2, MnO_2, Co_3O_4, and NiO) are well investigated as pseudo-capacitive for their multi-electron transfer during fast faradic reactions [14-17]. Particularly, cobalt (II, III) oxide (Co_3O_4) which has a theoretical specific capacitance (SC) of 3560 $F{\cdot}g^{-1}$ has been considered as an excellent electroactive material for its low cost, high redox activity, great reversibility, and environmental friendliness [18-20]. Up to now, the observed SCs of Co_3O_4 are much lower than its theoretical value. Therefore, it is still a challenge and necessary to develop efficient but simple ways to enhance the utilization of electroactive Co_3O_4, particularly at high rates. To satisfy this urgent requirement, several researches have focused on the Co_3O_4-Carbon materials, because of the carbon materials can combined with other active materials to enhance the electrochemical performance of supercapacitors [21-25].

In the last two decades, porous coordination polymers (PCPs) or metal-organic frameworks (MOFs), which are newly emerging porous materials with multiple functionalities, have attracted much attention because of their high surface area, tunable porosity, and wide potential applications in gas storage and separation, catalysis, sensing, recognition, drug delivery, and so on [26-28]. In the last five years, PCPs or MOFs have been proven to be promising precursors or sacrificial templates to construct metal oxides or metal oxides-carbons composites via thermal conversion [29-31]. Compared with other templates, the pore characteristics and the morphologies of PCPs or MOFs could be preserved in the obtained materials. More importantly, the materials derived from PCPs or MOFs show promising applications in energy and environmental fields such as LIB, capacitors, water treatment, and so on [32-34].

Herein, we present an approach of using mesoporous octahedral Co_3O_4 @ carbon composites derived from PCPs as electrode material for supercapacitors. Up to now, only a few studies on the construction of metallic cobalt-carbon composites derived from PCPs or MOFs have been reported. In 2015, Wei and

[a] Research Institute of Special Chemicals, Taiyuan University of Technology, Taiyuan, 030024 (China), E-mail: jpli211@hotmail.com.
† Electronic Supplementary Information (ESI) available: PXRD of ZSA-1, EDX, cyclingperformance, some SEM and TEM results. See DOI: 10.1039/x0xx00000x

his co-workers reported a metallic cobalt-carbon composite with good performance in supercapacitors, which was synthesized by ZIF-67 as precursors via a one-step thermal decomposition process. The sample exhibits specific capacitance of 144.5 $F \cdot g^{-1}$ at current density of 0.5 $A \cdot g^{-1}$ and capacitance retention rate of 96.5% at current density of 2 $A \cdot g^{-1}$. The excellent performance of the composites was attributed to the well-organized interleaved structure consisting of metallic cobalt and carbon, and the composites can greatly increase the electrode/electrolyte interface, and facilitation diffusion [35].

In this work, we have elaborately chosen chemically and thermally robust as well as highly porous zeolite-like PCPs (ZSA-1) as precursors. Accordingly, ZSA-1 has formed by bridging 4, 5-imidazoledicarboxylic acid (ImDC), 1, 2-propanediamine (1, 2-PDA) and cobalt cations resulting in *gismondine* topology with an average pore size of 5.3 Å. Therefore, ZSA-1 has been regarded as the suitable model to explore the fabrication and potential applications of the metallic cobalt-carbon composites heterostructure.

Experimental

Materials and methods

All the reagents were obtained from commercial sources and used without further purification. All used gases are pure gases (N_2: 99.99 %). A tube furnace (ZKGL1400) was used for carbonization. Powder X-ray diffraction (PXRD) were performed on a Rigaku Mini FlexII X-ray diffractometerusing Cu-Kα_1 radiation (30 kV, 15 mA, λ = 0.15418 nm) with a step size of 0.01° and a scanning rate of 2° min^{-1}. Thermogravimetric analyses were performed on NETZSCH STA 449F5 thermogravimetric analyser with a heating rate of 10 °C·min^{-1}. Scanning electron microscopic (SEM) analyses and energy dispersive X-ray spectroscopy (EDX) data were acquired on a Hitachi SU8010 and an IXRF Systems SDD2610-A550I, respectively. Transmission electron microscopy (TEM) images were captured on the JEM-2100F microscope at an acceleration voltage of 200 kV. A Raman spectrum was recorded on a RENISHAW Invia Raman microscope. Raman system was under room temperature at an excitation wavelength of 514 nm. The surface area measurement was performed with N_2 adsorption-desorption isotherms at liquid nitrogen temperature (77 K) using automatic volumetric adsorption equipment (Quanta chrome Autosorb IQ) after dehydration under vacuum at 200 °C for 2 h. The surface area was calculated using the BET method. Pore size distribution was performed on a Micromeritics ASAP-2460.

Synthesis of ZSA-1

ZSA-1($|(H_2O)_{28}|[Co_4(C_5HN_2O_4)_4(C_3H_{10}N_2)_4]$) was first prepared based on the reported procedures [36]. In a typical synthesis, a mixture of 4, 5-Imidazoledicarboxylic acid (0.040 g, 0.25 mmol), $Co(CH_3COO)_2 \cdot 4H_2O$ (0.060 g, 0.25 mmol), 1, 2-PDA (0.060 mL), and H_2O (3 mL) were sealed in a Teflon-lined stainless steel autoclave, heated at 120 °C for 20 h, and then cooled to room temperature. The red octahedral crystals were isolated, washed with distilled water, and dried in air.

Synthesis of mesoporous Co_3O_4 @ carbon composites

Mesoporous Co_3O_4 @ carbon composites were synthesized by carbonization of ZSA-1 under a flow of nitrogen gas at temperature of 600 °C. Typically, ZSA-1 octahedral crystals about 500 mg was homogeneously dispersed in a ceramic boat. The sample was exposed to a flow of nitrogen (100 mL·min^{-1}) at room temperature for an hour and afterward the furnace was heated to the targeted carbonation temperature with a heating rate of 2 °C·min^{-1}. After reaching the targeted temperature, it was immediately cooled down to room temperature with a cooling rate of 2 °C·min^{-1}. The resultant black powders were collected.

Synthesis of bare Co_3O_4 particles

Bare Co_3O_4 particles were obtained by annealed ZSA-1 directly in ambient atmosphere at 600 °C with a heating rate of 2 °C·min^{-1}. After reaching the targeted temperature, it was immediately cooled down to room temperature with a cooling rate of 2 °C·min^{-1}. The resultant black powders were collected.

Electrochemical capacitor measurements

All electrochemical measurements were carried out using an electrochemical work station (CHI660E, Shanghai, China) in a three electrode cell system at room temperature. The working electrodes of Co_3O_4 @ carbon composites, ZSA-1 and bare Co_3O_4 particles were all prepared according to the following procedure: 40 mg (80%) active substance, 5 mg (10%) acetylene black as the conducting agent and 5 mg (10%) polytetrafluoroethylene (5%) as a binder were homogeneously mixed with a few drops of ethanol and ultrasound in a vial until homogeneous black slurry was obtained. After that, the prepared mixed slurry was dropped onto the nickel foam with the geometric surface area of 1 cm^2 to form a film. The film was dried at 80 °C for 12 h, then was pressed under 10 MPa. The mass load of the electrodes was about 3.92, 2.56, and 6.88 $mg \cdot cm^2$ for Co_3O_4 @ carbon composites, ZSA-1 and bare Co_3O_4 particles, respectively. An Hg/HgO electrode was employed as the reference electrode, and a platinum network electrode was used as the counter electrode. 6 M KOH solutions were adopted as electrolyte in the study. Cyclic voltammetry (CV) were measured within the potential range from 0 to 0.50 V versus the Hg/HgO electrode at various scan rates. The constant current galvanostatic charge-discharge tests were carried out between 0 and 0.48 V at various current densities ranging from 0.2 to 5 $A \cdot g^{-1}$. The SC of the electrode has been calculated according to $C = I \times \Delta t / (\Delta V \times m)$, I is the constant discharge current, Δt is the discharge time, ΔV is the potential drop during discharge, and m represents the mass of the active substance within the working electrode [30].

Results and discussions

The phase composition of the precursors was investigated by PXRD. Fig.**S1a** shows the PXRD pattern of the obtained precursors while Fig. **S1b** displays the PXRD pattern of ZSA-1 which is converted from ".cif" file from the literature using materials studio software [36]. By comparing the two PXRD patterns, it can be easily deduced that the obtained precursors were ZSA-1. ZSA-1 crystallizes in the tetragonal $I4_1/amd$ space group with the cell length ($a = b$ = 18.057(3) Å, c = 23.058(5) Å) and cell angle ($\alpha = \beta = \gamma = 90^o$). Fig. **1a** presents the schematic representations of the metal-organic square

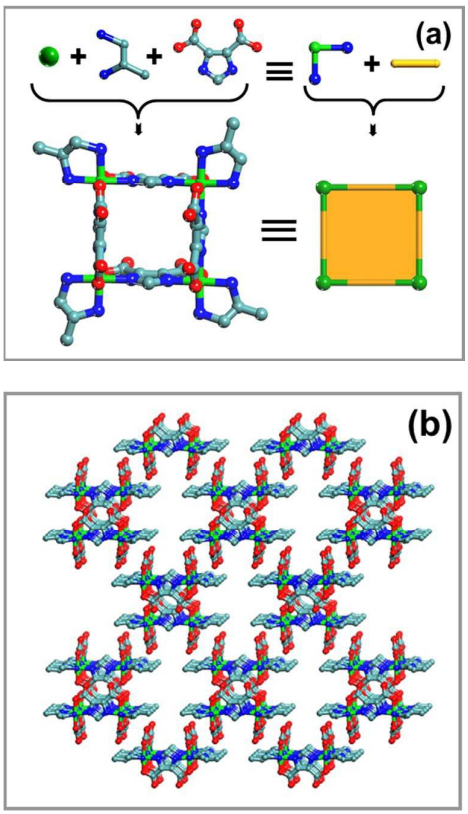

Fig. 1. (a) The ball-and-stick and schematic representations of the metal-organic square secondary building unit. (b) The stick model of the 3D framework showing the orthogonal openings.

secondary building unit in ZSA-1. And Fig. **1b** displays space-filling representations of the framework of ZSA-1 showing two orthogonal channels along ***a*** and ***b*** axes. The PXRD analyses of Co_3O_4 @ carbon composites and bare Co_3O_4 particles can be unambiguously indexed to the cubic spinel Co_3O_4, which confirms the standard spectrum of Co_3O_4 (JCPDS card no.43-1003, space group: *F*d3m (227), a = 8.084 Å) (Fig. **2a**). The diffraction peaks at 19.00°, 31.27°, 36.85°, 38.55°, 44.81°, 59.35° and 65.23° can be indexed as the (111), (220), (311), (222), (400), (511) and (440) crystal planes of Co_3O_4, respectively. Especially, there is a broad peak at approximately 2θ = 25° of the PXRD spectrum of Co_3O_4 @ carbon composites, which is the typical spectrum of carbon substrate. Fig. **2b** shows the Raman spectrum of the composites, carbon and pure Co_3O_4 in detail over the range of 0 to 2000 cm^{-1}, where the vibrational peaks at approximately 1346 and 1591 cm^{-1} can be attributed to the D and G bands [37]. The peaks at 479, 527 and 688 cm^{-1} can be assigned to classical vibration modes Eg, F2g, and A1g of cubic spinel Co_3O_4, respectively [38, 39].

The sample of ZSA-1 has been activated under vacuum at 200 °C for 2 hours before thermogravimetric analysis measurement. The profile for activated ZSA-1 indicates that the guest water molecules captured in the pore have been mostly removed, and the framework of ZSA-1 was stable to 300°C. As shown in Fig.**S2**, thermogravimetric analysis for activated ZSA-1 under N_2 shows a two-step weight loss of 68.32 % between 300 and 473 °C, which

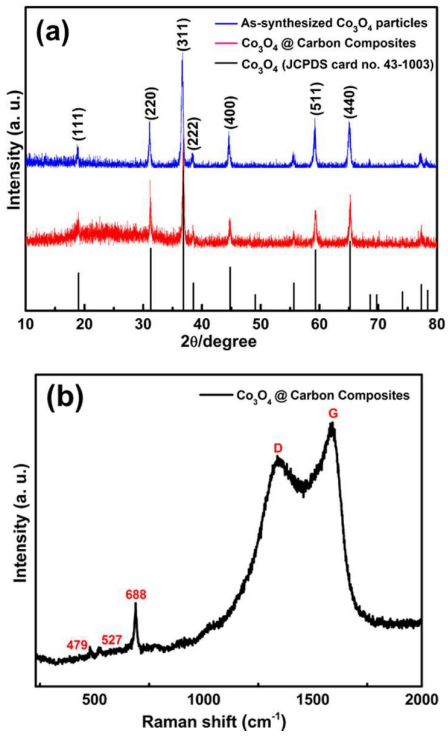

Fig. 2. (a) PXRD patterns of the Co_3O_4 @ carbon composites and the as-synthesized Co_3O_4 particles. (b) Raman spectra of the Co_3O_4 @ carbon composites.

should be corresponded to the decomposition of the ImDC ligands and 1, 2-PDA (calcd: 79.38 %). During the heat treatment under N_2 atmospheres, organic ligands thermally carbonized into carbon, and parts of organic ligands decomposed and evaporated in the form of small molecules (e.g., H_2, N_2, CO_2, CO) [43-45]. The residual weight of 31.68 % corresponds to Co_3O_4 @ Carbon composites. In addition, thermogravimetric analysis for Co_3O_4 @ Carbon composites under air shows a weight loss of 28.13 % corresponding to the release of carbon. The residual weight of 71.87 % should be Co_3O_4 particles.

The morphologies have been successfully maintained during the process of calcination, and the Co_3O_4 @ carbon composites also have octahedral morphologies (See Fig. **S3, 3a**). The sizes of the as-synthesized octahedrons are ranged in 300-500 nm, which are smaller than the precursors ZSA-1. Besides, the irregular particle agglomerates are observed in Fig. **3b**, indicating that the obtained octahedrons are actually composed of numerous nanoparticles with an average size of 10 nm, and these particles undergone further aggregation to form agglomerate octahedrons. The EDX spectrum confirms the existence of C, O, and Co, which indicates that the composite **derived** from ZSA-1, might be cobalt oxide and carbon substance (Fig. **S4**). Furthermore, HRTEM examination was carried out to determine the crystal orientation feature of the composites. It is observed that Co_3O_4 have been uniformly loaded on the surface of carbon substrates forming nanoparticles, moreover, the sizes of circular particle are ranged from 10 nm to 20 nm, which are in good agreement with the SEM results (See Fig. **S5**). The HRTEM image of a single particle displays clear lattice fringes with lattices spacing of about 0.466 nm and 0.233 nm, corresponding to the d_{111} and d_{222}

Journal Name

COMMUNICATION

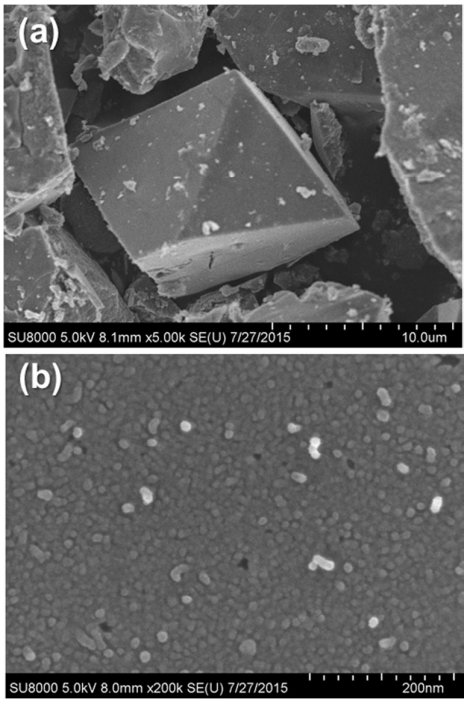

Fig. 3. (a) and (b) SEM images for the Co_3O_4 @ carbon composites.

plane of cubic Co_3O_4 structure respectively in Fig. 4. The sizes of the as-synthesized Co_3O_4 particles are ranged from 20 nm to 50 nm, which are much larger than the Co_3O_4 particles in Co_3O_4 @ Carbon composites (Fig. S6).

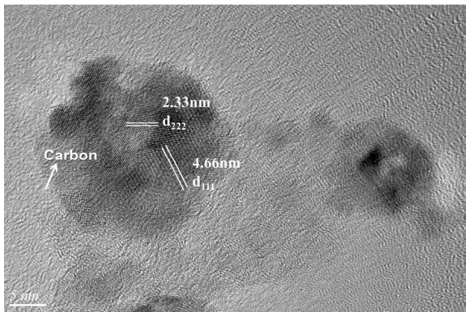

Fig. 4. HRTEM images for the nanoparticles of Co_3O_4 @ carbon composites.

Isothermal N_2 adsorption-desorption analyses were performed to further evaluate the porous features of Co_3O_4 @ carbon composites. The N_2 adsorption-desorption isotherms at 77 K and the Barrett-Joyner-Halenda (BJH) adsorption pore size

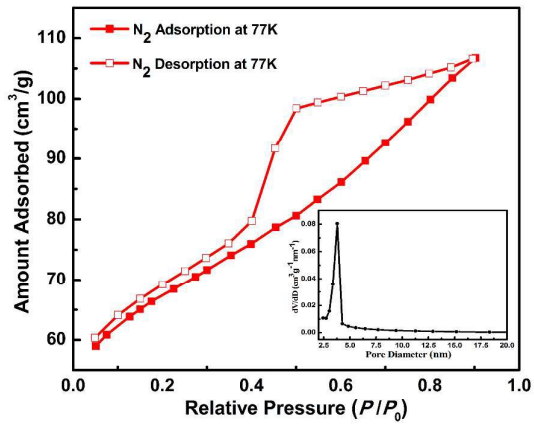

Fig. 5. N_2 sorption-desorption isotherms, and the inset shows pore size distribution of the composites.

distribution plot of Co_3O_4 @ carbon composites are shown in Fig. 5. The nitrogen adsorption isotherm is a typical IV type curve. The loop in the nitrogen adsorption isotherm further suggests its uniform mesoporous structure. The specific BET surface area of the Co_3O_4 @ carbon composites is 216 $m^2 \cdot g^{-1}$. In addition, according to the corresponding BJH pore size distribution curve, the average pore size is 3.6 nm.

To explore the potential applications of Co_3O_4 @ carbon composites, the samples were fabricated into supercapacitors electrodes and characterized with cyclic voltammetry (CV) and galvanostatic charge-discharge measurements. As shown in Fig. 6, only an oxidation peak (A) and a reduction peak (C) have been found in each CV curve. It is because that two oxidation peaks (A1 and A2) and two reduction peaks (C1 and C2) have merged with each other, then leaving one oxidation peak (A) and one reduction (C) peak in the present case. The phenomenon is consistent with

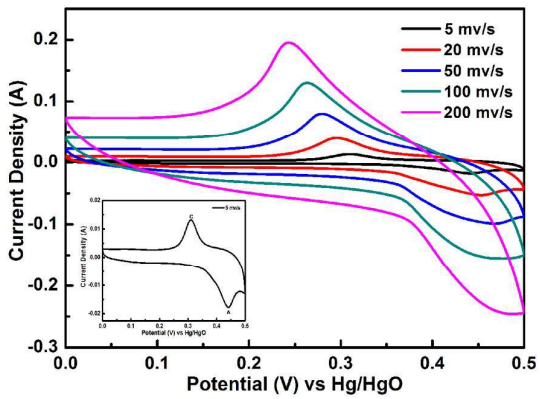

Fig. 6. Cyclic voltammetry curves measured at sweep rates of 5, 20, 50, 100, and 200 $mV \cdot s^{-1}$.

some relevant studies [32, 40]. The pair of well-defined redox peaks is observed within the range 0.0-0.5 V, which corresponds to the reversible conversion between different cobalt oxidation states. It reveals the pseudo-capacitive property of Co_3O_4 @ carbon composites and shows the surface redox mechanism of Co^{2+} to Co^{3+} on the surface of Co_3O_4 @ carbon composites according to the following equation [41]:

$$Co_3O_4 + OH^{-1} + H_2O \rightarrow 3CoOOH + e^{-1} \quad (1)$$

$$CoOOH + OH^{-1} = CoO_2 + H_2O + e^{-1} \quad (2)$$

To further evaluate the application potential of composites as electrodes for ECs, galvanostatic charge-discharge measurements were carried out (Fig. 7). The potential-time curves are nearly symmetrical, which indicates Co_3O_4 @ carbon composites electrode has electrochemical capability and the redox process is reversible. The specific capacitance was calculated from the galvanostatic charge-discharge curves. The SC value of the composites electrode is 205.4, 194.8, 183.1, 172.9, 151.3 $F{\cdot}g^{-1}$ at the current density of 0.2, 0.5, 1, 2, 5 $A{\cdot}g^{-1}$, respectively. It has been found that the capacitance decreased with an increase in discharge current density, which was the result of the resistance increase in electrode and the insufficient faradic redox reaction under higher current

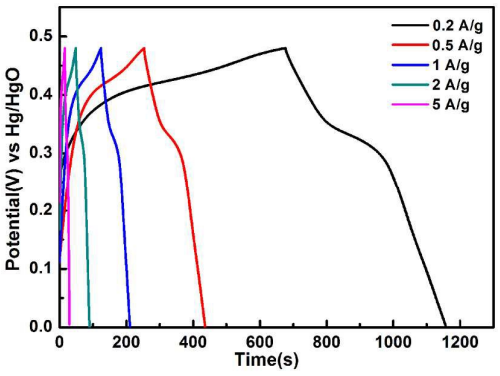

Fig. 7. Galvanostatic charge-discharge curves at different current densities.

density [42]. Figure S7 presents the SC retention of 73.66 % at 5 $A{\cdot}g^{-1}$. Furthermore, the cycle charge-discharge tests have been investigated at constant current density 2 $A{\cdot}g^{-1}$. The Co_3O_4 @ carbon composites electrode exhibits an electrochemical stability, and the capacitance has lost after 500 cycles was 11.1 % (Fig. S8). In addition, the electrochemical properties of ZSA-1 and bare Co_3O_4 particles were also investigated by CV and galvanostatic charge-discharge techniques, respectively. The CV curves suggest the pseudo-capacitive properties of ZSA-1 and bare Co_3O_4 particles (Fig. S9, S11). The potential-time curves are all nearly symmetrical, which indicate ZSA-1 and bare Co_3O_4 particles electrodes have electrochemical capability and the redox processes are reversible. Accordingly, the SC value of ZSA-1 electrode is 74, 61.8, 50.8, 41, 30.4 $F{\cdot}g^{-1}$ at the current density of 0.2, 0.5, 1, 2, 5 $A{\cdot}g^{-1}$, respectively. And, the SC value of bare Co_3O_4 particles electrode is 58.2, 54, 52.3, 48.2, 41.4 $F{\cdot}g^{-1}$ at the current density of 0.2, 0.5, 1, 2, 5 $A{\cdot}g^{-1}$, respectively. As a result, the pseudo-capacitance retentions of Co_3O_4 @ carbon composites are much higher than ZSA-1 and bare Co_3O_4 particles. The improvement of the pseudo-capacitive performance has been attributed to the intimate integration between the porous carbon substance with good electronic conductivity and the Co_3O_4 particles array directly on it [16, 17, 27].

Conclusions

In summary, we have successfully developed a facile route to synthesize mesoporous Co_3O_4 @ carbon composites by one-step carbonization of microporous cobalt-based coordination polymers ZSA-1. The original octahedral shape of the precursors ZSA-1 has been well preserved in the as-obtained Co_3O_4 @ carbon composites. The electrochemical tests show that Co_3O_4 @ carbon composites exhibiting a specific capacitance of 205.4 $F{\cdot}g^{-1}$ at 0.2 $A{\cdot}g^{-1}$ and a specific capacitance retention rate of 73.66 % when the current density is increased from 0.2 to 5 $A{\cdot}g^{-1}$. The porous carbon substance in the Co_3O_4 @ carbon composites has been responsible for the improvement of the pseudo-capacitive properties. The simple thermal treatment method has be anticipated to be applicable to other PCPs, and the electrochemical performance of the resulting hybrids could be improved by enhancing the BET surface areas and fine tuning of crystallite sizes and morphologies of the PCPs precursors as well as the thermal-treatment conditions. What's more, cobalt-oxide @ carbon composites not only can be applied in capacitor electrodes, but also can be used in other energy storage devices (such as lithium ion battery), catalytic materials, and magnetic materials and so on.

Acknowledgements

The authors acknowledge the financial support of the Natural Science Foundation of China (Grant Nos. 51203109, 21136007), the National Key Basic Research Program of China (Nos. 2014CB260402), the projectssupported by SXNSF (2013021008-2, 2015021058),the Youth Foundation of Taiyuan University of Technology (Nos. 2014YQ003).

Notes and references

[1] L. Zhang, H. B. Wu, S. Madhavi, H. H. Hng and X. W. Lou, *Journal of the American Chemical Society,*2012, **134**, 17388-17391.

[2] A. S. Arico, P. Bruce, B. Scrosati, J. M. Tarascon and W. Van Schalkwijk, *Nature Materials,*2005, **4**, 366-377.

[3] P. Simon and Y. Gogotsi, *Nature Materials*, 2008, **7**, 845-854.

[4] G. Wang, L. Zhang and J. Zhang, *Chemical Society Reviews*, 2012, **41**, 797-828.

[5] C. Largeot, C. Portet, J. Chmiola, P. L. Taberna, Y. Gogotsi and P. Simon, *Journal of the American Chemical Society,* 2008, **130**, 2730-2731.

[6] L. Wei, M. Sevilla, A. B. Fuertes, R. Mokaya and G. Yushin, *Advanced Functional Materials,* 2012, **22**, 827-834.

[7] C. W. Huang, C. A. Wu, S. S. Hou, P. L. Kuo, C. T. Hsieh and H. Teng, *Advanced Functional Materials*, 2012, **22**, 4677-4685.

[8] G. Pan, X. Xia, F. Cao, P. Tang and H. Chen, *Electrochemistry Communications*, 2013, **34**, 146-149.

[9] G. Wang, X. Lu, Y. Ling, T. Zhai, H. Wang, Y. Tong and Y. Li, *ACS Nano,* 2012, **6**, 10296-10302.

[10] J. H. Kim, S. H. Kang, K. Zhu, J. Y. Kim, N. R. Neale and A. J. Frank, *Chemical Communications*, 2011, **47**, 5214-5216.
[11] J. Han, G. Xu, H. Dou and D. R. MacFarlane, *Chemistry-A European Journal*, 2015, **21**, 2310-2314.
[12] Y. Zhu, S. Murali, M. D. Stoller, K. Ganesh, W. Cai, P. J. Ferreira, A. Pirkle, R. M. Wallace, K. A. Cychosz and M. Thommes, *Science*, 2011, **332**, 1537-1541.
[13] L. L. Zhang and X. Zhao, *Chemical Society Reviews,* 2009, **38**, 2520-2531.
[14] M. G. Jeong, K. Zhuo, S. Cherevko, W. J. Kim and C. H. Chung, *Journal of Power Sources*, 2013, **244**, 806-811.
[15] W. Wei, X. Cui, W. Chen and D. G. Ivey, *Chemical Society Reviews*, 2011, **40**, 1697-1721.
[16] Y. Zhang, L. Li, S. Shi, Q. Xiong, X. Zhao, X. Wang, C. Gu and J. Tu, *Journal of Power Sources*, 2014, **256**, 200-205.
[17] C. Zhang, L. Qian, K. Zhang, S. Yuan, J. Xiao and S. Wang, *Journal of Materials Chemistry A*, 2015, **3**, 10519-10525.
[18] X. H. Xia, J. P. Tu, X. L. Wang, C. D. Gu, X. B. Zhao, *Chem. Commun.*, 2011, **47**, 5786-5788.
[19] L. R. Hou, C. Z. Yuan, L. Yang, L. F. Shen, F. Zhang, X. G. Zhang, *RSC Adv.*, 2011, **1**, 1521-1526.
[20] Y. Y. Liang, M. G. Schwab, L. J. Zhi, K. U. Mugnaioli, X. L. Feng, K. Müllen, *J. Am. Chem. Soc.*, 2010, **132**, 15030-15037.
[21] C. Yuan, L. Yang, L. Hou, J. Li, Y. Sun, X. Zhang, L. Shen, X. Lu, S. Xiong and X. W. D. Lou, *Advanced Functional Materials*, 2012, **22**, 2560-2566.
[22] X. Xia, J. Tu, Y. Mai, R. Chen, X. Wang, C. Gu and X. Zhao, *Chemistry-A European Journal,* 2011, **17**, 10898-10905.
[23] Q. Guan, J. Cheng, B. Wang, W. Ni, G. Gu, X. Li, L. Huang, G. Yang and F. Nie, *ACS Appl. Mater. Interfaces,* 2014, **6**, 7626-7632.
[24] L. Q. Mai, A. Minhas-Khan, X. Tian, K. M. Hercule, Y. L. Zhao, X. Lin and X. Xu, *Nat. Commun.*, 2013, **4**, 2923-2929.
[25] M. F. de Volder, S. H. Tawfick, R. H. Baughman and A. J. Hart, *Science*, 2013, **339**, 535-539.
[26] J. A. Mason, J. Oktawiec, M. K. Taylor, M. R. Hudson, J. Rodriguez, J. E. Bachman, M. I. Gonzalez, A. Cervellino, A. Guagliardi and C. M. Brown, *Nature*, 2015, **527**, 357-361.
[27] Y. He, B. Li, M. O'Keeffe and B. Chen, *Chemical Society Reviews*, 2014, **43**, 5618-5656.
[28] Z. Zhang and M. J. Zaworotko, *Chemical Society Reviews*, 2014, **43**, 5444-5455.
[29] W. Du, R. Liu, Y. Jiang, Q. Lu, Y. Fan and F. Gao, *Journal of Power Sources*, 2013, **227**, 101-105.
[30] F. Meng, Z. Fang, Z. Li, W. Xu, M. Wang, Y. Liu, J. Zhang, W. Wang, D. Zhao and X. Guo, *Journal of Materials Chemistry A,* 2013, **1**, 7235-7241.
[31] J. K. Sun and Q. Xu, *Energy & Environmental Science,* 2014, **7**, 2071-2100.
[32] Y. Z. Zhang, Y. Wang, Y. L. Xie, T. Cheng, W. Y. Lai, H. Pang and W. Huang, *Nanoscale*, 2014, **6**, 14354-14359.
[33] R. Wu, X. Qian, X. Rui, H. Liu, B. Yadian, K. Zhou, J. Wei, Q. Yan, X. Q. Feng and Y. Long, *Small*, 2014, **10**, 1932-1938.
[34] K. Y. A. Lin and F. K. Hsu, RSC Advances, 2015, 5, 50790-50800.
[35] F. Wei, J. Jiang, G. Yu and Y. Sui, *Materials Letters*, 2015, **146**, 20-22.
[36] S. Wang, T. Zhao, G. Li, L. Wojtas, Q. Huo, M. Eddaoudi and Y. Liu, *Journal of the American Chemical Society,* 2010, **132**, 18038-18041.
[37] T. Kuila, S. Bose, A. K. Mishra, P. Khanra, N. H. Kim and J. H. Lee, *Progress in Materials Science*, 2012, **57**, 1061-1105.
[38] Y. Liu, W. Yu, L. Hou, G. He and Z. Zhu, *RSC Advances*, 2015, **5,** 75105-75110.
[39] R. Rakhi, W. Chen, D. Cha and H. Alshareef, *Nano Letters*, 2012, **12**, 2559-2567.
[40] M. Kruk and M. Jaroniec, *Chemistry of Materials,* 2001, **13**, 3169-3183.
[41] J. Liu, J. Jiang, C. Cheng, H. Li, J. Zhang, H. Gong and H. J. Fan, *Advanced Materials*, 2011, **23**, 2076-2081.
[42] Y. G. Wang and Y. Y. Xia, *Journal of the Electrochemical Society,* 2006, **153,** A450-A454.
[43] S. J. Yang, T. Kim, J. H. Im, Y. S. Kim, K. Lee, H. Jung and C. R. Park, *Chem. Mater.,* 2012, **24**, 464-470.
[44] J. Tang, R. R. Salunkhe, J. Liu, N. L. Torad, M. Imura, S. Furukawa and Y. Yamauchi, *J. Am. Chem. Soc.,* 2015, **137**, 1572-1580.
[45] N. L. Torad, M. Hu, S. Ishihara, H. Sukegawa, A. A. Belik, M. Imura, K. Ariga, Y. Sakka and Y. Yamauchi, *Small*, 2014, **10**, 2096-2107.

